On the Impact of Dzhanibekov's Effect on Earth Dynamics: Scaled Experiments with Free-falling Rotating Bodies

By Mateo Guzmán Subiría

Supervised by Dr Irena Vorgul

School of Physics and Astronomy, University of St Andrews, UK

ACKNOWLEDGMENTS

I would like to thank my supervisor, Dr Irena Vorgul, for giving me the opportunity to work on this project. Appreciation is given to my fellow Laidlaw scholars, my friends, and my girlfriend Natalia for providing me with emotional support, and encouragement. A special mention goes to my friend Nikko for letting me use his camera for the project and offering creative solutions for my technical problems. Finally, I thank Lord Laidlaw and the Laidlaw Foundation for funding this project and allowing me to partake in the Scholarship Programme.

OVERVIEW

The project explores Dzhanibekov's effect and a possibility of it influencing Earth dynamics. We suggest a more general theory than the existing explanation in terms of the intermediate axis theorem, showing that the latter is only a particular case of Dzhanibekov's effect. The main part of the project was building an experimental set up and using it to explore the effect on rotating bodies in free fall (to exclude the influence of gravity).

This was a pilot research in a novel area, hence being done from scratch. Each consecutive step depended on a previous one, so the scope of the project was continuously adjusted in line with obtained results, experience, and technical limitations. That brought in real life experience in research[1] and taught me many useful skills, including reflection, flexibility, positive thinking, enquiring, determination, and lateral thinking.

We present the devices and their function, and the observations obtained.

[1] Recall a quote by Albert Einstein, "If I knew what I was doing it would not be called research, would it?"

1. INTRODUCTION & THEORY

1.1 Dzhanibekov's effect

Dzhanibekov's effect takes its name after its discoverer, cosmonaut Vladimir Dzhanibekov, who first witnessed it in space aboard the MIR space station in 1985. After flicking a wingnut to release it, he observed that, under microgravity, the nut travelled in a straight line rotating about the nut axis. Then, suddenly and without a noticeable cause, it flipped 180° along the nut axis. These flips repeated themselves over regular time intervals[2]. The images in figure 1, taken from a video recorded aboard the International Space Station, illustrate Dzhanibekov's effect[3].

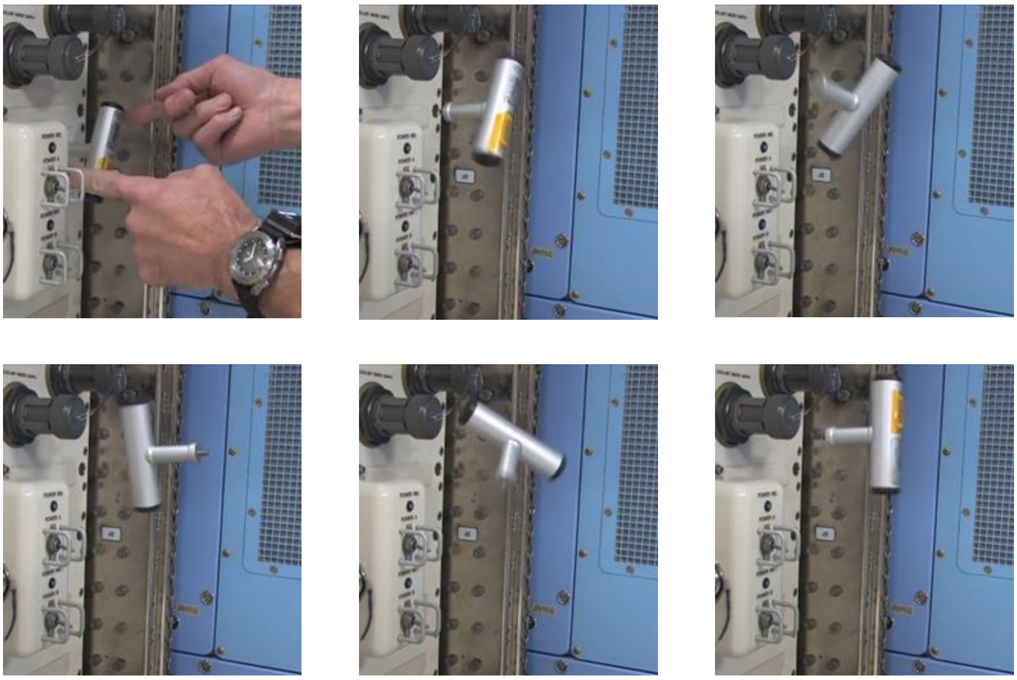

Figure 1: Dzhanibekov's effect on a T-handle in microgravity. Clips from the original video are chronologically ordered from left to right and from top to bottom. Taken from YouTube, *2009.*

The conventional explanation is in terms of the Intermediate Axis Theorem (IAT) (also called the Tennis Racket Theorem). We say an object twists, spins, rotates, etc. about an axis (e.g. z in fig. 2) if it rotates on a plane perpendicular to said axis[4]. Asymmetric three-dimensional objects can be assigned three different principal moments of inertia (MOIs) – a quantity that determines how much an object's rotational motion changes in response to an applied force (torque) – along

---

[2] Petrov, A. G. and Volodin, S. E. Janibekov's Effect and the Laws of Mechanics. *Doklady Akademii Nauk*, 2013; 4 (**Vol. 451**), pp. 399–403. DOI: 10.1134/S1028335813080041

[3] Plasma Ben. Published 3 of March 2009. Dancing T-handle in zero-g, HD. [Video]. YouTube.com. https://www.youtube.com/watch?v=1n-HMSCDYtM

[4] Gorbunov, A., Kozhevnikov, M., Olesya, B. and Royan, J. The Role of Immersivity in Three-Dimensional Mental Rotation. *Design Computing and Cognition*, 2008, pp.143-157. DOI: 10.1007/978-1-4020-8728-8_8

three perpendicular (principal) axes labelled minor, intermediate, and major in order of increasing associated MOI. The IAT states that an asymmetrical rotating object will spin stably around the minor and major axes, but, if it spins around the intermediate one, its motion will perform a periodic strange movement due to instability in its spin[5] resulting in a twist about the other axes. This is because the axis of rotation does not exactly align with the intermediate principal axis or, if it did, any small disturbance would make it differ just slightly and it would be enough to kick off the effect.

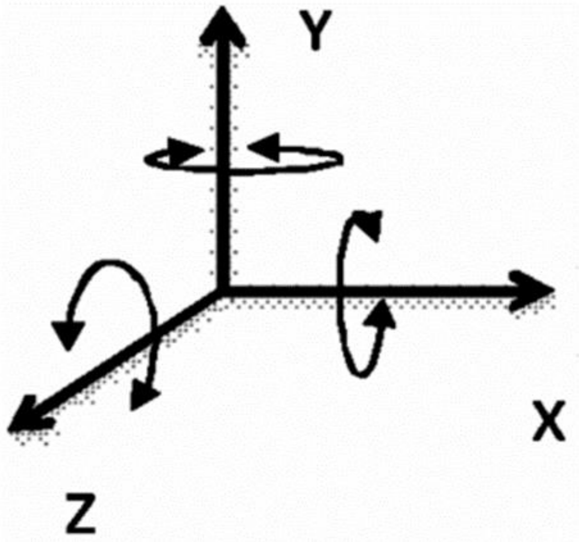

Figure 2: Rotation axes. Taken from Design Computing and Cognition*, 2008.*

We describe this motion with Euler's Equations of Motion for a rigid body[6]:

$$\begin{aligned} I_1\dot{\omega}_1 + (I_3 - I_2)\omega_3\omega_2 &= M_1 \\ I_2\dot{\omega}_2 + (I_1 - I_3)\omega_1\omega_3 &= M_2 \\ I_3\dot{\omega}_3 + (I_2 - I_1)\omega_2\omega_1 &= M_3 \end{aligned} \tag{1}$$

Here, $I_{1,2,3}$ are the MOI corresponding to the minor (1), intermediate (2), and major (3) principal axes; $\omega_{1,2,3}$ are the time-changing angular velocities about the principal axes, $\dot{\omega}_{1,2,3} \equiv \frac{d\omega_{1,2,3}}{dt}$ are the changes in $\omega_{1,2,3}$ with respect to time i.e., the angular accelerations, and $M_{1,2,3}$ are the torques (rotational effect from an applied force) about the principal axes.

[5] Garelli, L., Storti, M. and Trivisonno, N. The Tennis Racket Theorem, Analysis and Numerical Simulation of the Intermediate Axis Theorem. *Mecánica Computacional*, 2021; (**Vol. 28**), pp. 1353-1365.
[6] Ashbaugh, M. S., Chicone, C. C., and Cushman, R. H. The Twisting Tennis Racket. *Journal of Dynamics and Differential Equations*, 1991; 1, (Vol. 3), pp 67-85. DOI: 10.1007/BF01049489

For a body spinning about axis 2, with $I_3 > I_2 > I_1$ and in force free motion ($M_1, M_2, M_3 = 0$), the equations give an exponential growth of ω_1 and ω_3 making this motion unstable[7].

(See appendix section 1 for the full derivation).

1.2 Quasi-linear solution

We show that, by considering Euler's equations in a less approximative manner, we can have Dzhanibekov's effect along other axes, given an adequate combination of parameters, and that the IAT is only a special case.

Here $I_1, I_2, I_3 = A, B, C$. We assume a rotation about the axis z corresponding to C, and effective torques with respect to the origin M_1, M_2, M_3 including torques from fictitious forces (centripetal force due to rotation). This accounts for any tiny deviation from a perfectly symmetric rotation, which is always the case, strictly speaking. Considering the non-zero torques and not ignoring the time-changing angular velocities produces a more advanced and precise theory compared to the IAT where those were ignored.

(See appendix section 2 for the full derivation).

$$\ddot{\omega_3} + D\omega_3 = \frac{\dot{M}_3}{C} - \frac{(B-A)(M_1 B\omega_2 + M_2 A\omega_1)}{ABC} \tag{2}$$

Where

$$D = -\frac{B-A}{ABC}\left[B(C-B){\omega_2}^2 - A(A-C){\omega_1}^2\right] \tag{3}$$

The LHS corresponds to a periodical motion if $D > 0$, describing ω_3 changing periodically between positive and negative values – a flip in rotation. The particular solutions $A > C > B$ and $B > C > A$ give $D > 0$ and correspond to the IAT. However, other solutions are possible.

Letting $A > B$ we need

$$B(C-B){\omega_2}^2 > A(C-A){\omega_1}^2 \tag{4}$$

For a given amount of angular momentum $L = I\omega$, an increase in I gives a decrease in ω. Similarly, kinetic energy $K = \frac{1}{2}I\omega^2 = \frac{L^2}{2I}$. Thus, for $A > B$, $K_1 < K_2$ and $\omega_1 < \omega_2$.

Hence, for $A > B$ we have $\omega_1 < \omega_2$, which makes the condition

[7] ThatsMaths. (2019). The Intermediate Axis Theorem. Accessed August 12th 2022 at https://thatsmaths.com/2019/12/12/the-intermediate-axis-theorem/

$$B(C - B) > A(C - A) \quad (5)$$

sufficient for the body to flip.

If $B > A$, we need

$$B(B - C){\omega_2}^2 > A(A - C){\omega_1}^2 \quad (6)$$

and similar conditions apply to the omegas.[8]

Thus, Dzhanibekov's effect can happen not only under IAT conditions, but also for the right combination of parameters when rotating around the major or minor axes. This result is important in application to Earth, which does not rotate around its intermediate axis.

1.3 The structure of the Earth

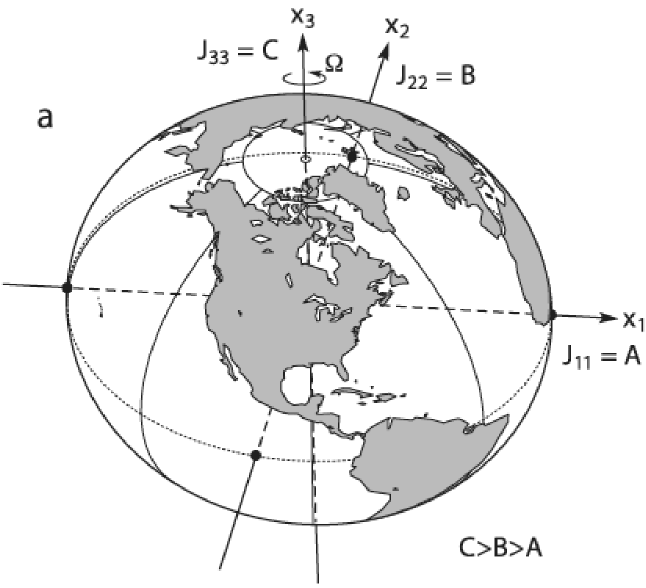

Figure 3: Earth's principal axes. Taken from Journal of Geophysical Research Atmospheres[9]*, 2010.*

[8] Daradich, A., Gomez, N., Matsuyama, I. and Mitrovica, J. X. The rotational stability of a triaxial ice-age Earth. *Journal of Geophysical Research Atmospheres,* 2010; BO5401, (**Vol. 115**). DOI: 10.1029/2009JB006564

[9] Daradich, A., Gomez, N., Matsuyama, I. and Mitrovica, J. X. The rotational stability of a triaxial ice-age Earth. *Journal of Geophysical Research Atmospheres,* 2010; BO5401, (**Vol. 115**). DOI: 10.1029/2009JB006564

The Earth is an asymmetric body with an uneven distribution of oceans and continents, extended at the Equator and it is even suggested it has an asymmetrically growing inner core[10]. Its rotation is continuously influenced by the 23° inclination of the axis with respect to the plane of its solar orbit and by the celestial bodies that surround it. Since the discovery of Dzhanibekov's effect the question of whether it could flip has been captivating, no less because of the catastrophe that would mean. Yet, the IAT would refute this since the Earth is rotating around the axis with the largest MOI.

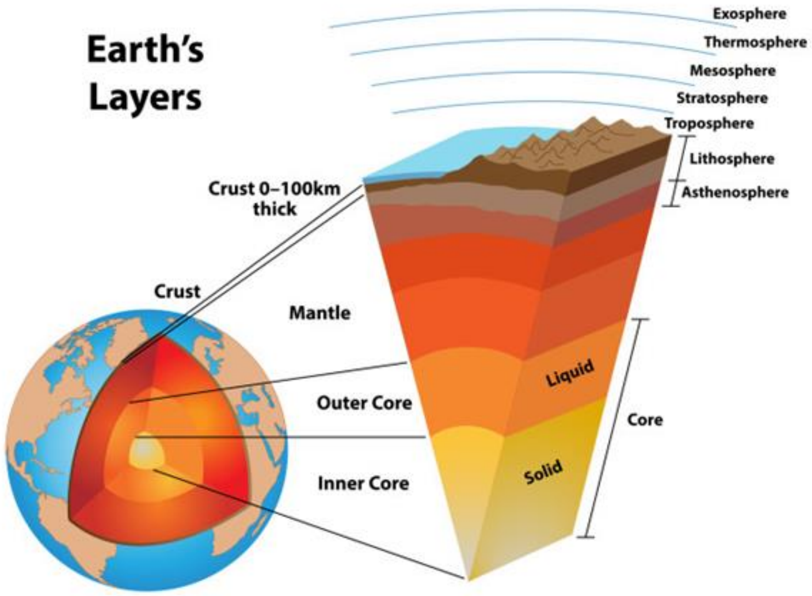

Figure 4: The Earth's structure. Taken from Astronomy[11], *2021.*

However, our new theory applied to the Earth's parameters[12]

A	8.0101×10^{37} kg m^2
B	8.0103×10^{37} kg m^2
C	8.0365×10^{37} kg m^2

shows that it could flip periodically if it were a rigid body since it has the right combination of parameters (fig.3). Here $B > A$, $B(B - C) \approx -0.2099$ and $A(A - C) \approx -0.2115$ so

[10] Chandler, B., Frost, D.A, Lasbleis, M. and Romanowicz, B. Dynamic history of the inner core constrained by seismic anisotropy. *Nature Geoscience,* 2021; (**Vol. 14**), pp 531–535. DOI: 10.1038/s41561-021-00761-w

[11] Sarkar, D. (2021). *Earth has been hiding a fifth layer in its inner core*. Astronomy. Accessed August 12th 2022 at https://astronomy.com/news/2021/03/earth-has-been-hiding-a-fifth-layer-in-its-inner-core

[12] Chen, W. and Shen, W.B. New estimates of the inertia tensor and rotation of the triaxial nonrigid Earth. *Journal of Geophysical Research*, 2010; B12, (**Vol. 115)**. DOI: 10.1029/2009JB007094

$$B(B-C)\omega_2{}^2 > A(A-C)\omega_1{}^2$$

is true for the right values of omegas.

Nevertheless, the Earth is far from being a solid. Its structure is multi-layered (fig. 4) and the outer core, making up about 30 % of Earth's mass[13], is liquid. We suggest that the co-rotating liquid part is likely to affect the effect of flipping, up to cancelling it.

1.4 The global magnetic field

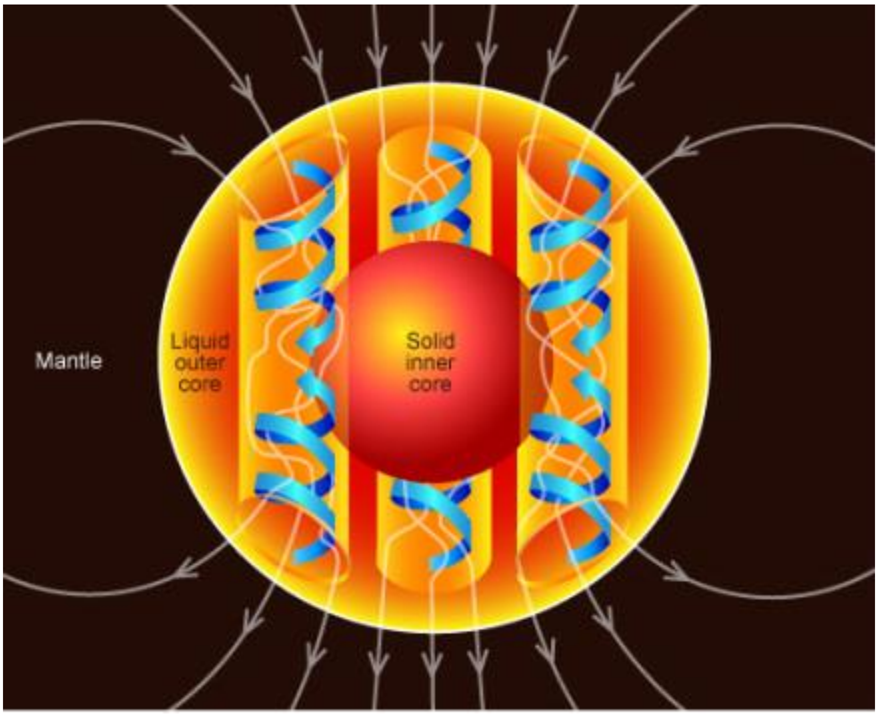

Figure 5: Diagram of magnetic field lines being created by fluid motion in the core. Taken from Harvard-Smithsonian Center for Astrophysics[16], *2016.*

In turn, the motion of the liquid iron in the outer core would be affected. According to dynamo theory (fig. 5), the motion of this conducting material creates our planet's magnetic field influenced mainly by convection processes and rotational forces[14]. In this manner, Dzhanibekov's effect could be influencing the terrestrial magnetic field's generation even if the full flip does not happen. It is worth highlighting that the global magnetic field is known to be

---

[13] GEOLOGYSCIENCE. The Earth's Layers. Accessed August 12th 2022 at https://geologyscience.com/geology-answer/the-earths-layers/

[14] The Editors of Encyclopaedia Britannica. *Dynamo Theory*. Accessed August 13th 2022 at https://www.britannica.com/science/dipolar-hypothesis

moving (fig. 6) and to have flipped (North and South poles exchanging places) several times in Earth's history[15], so, a relation between the two flipping effects is worth exploring.

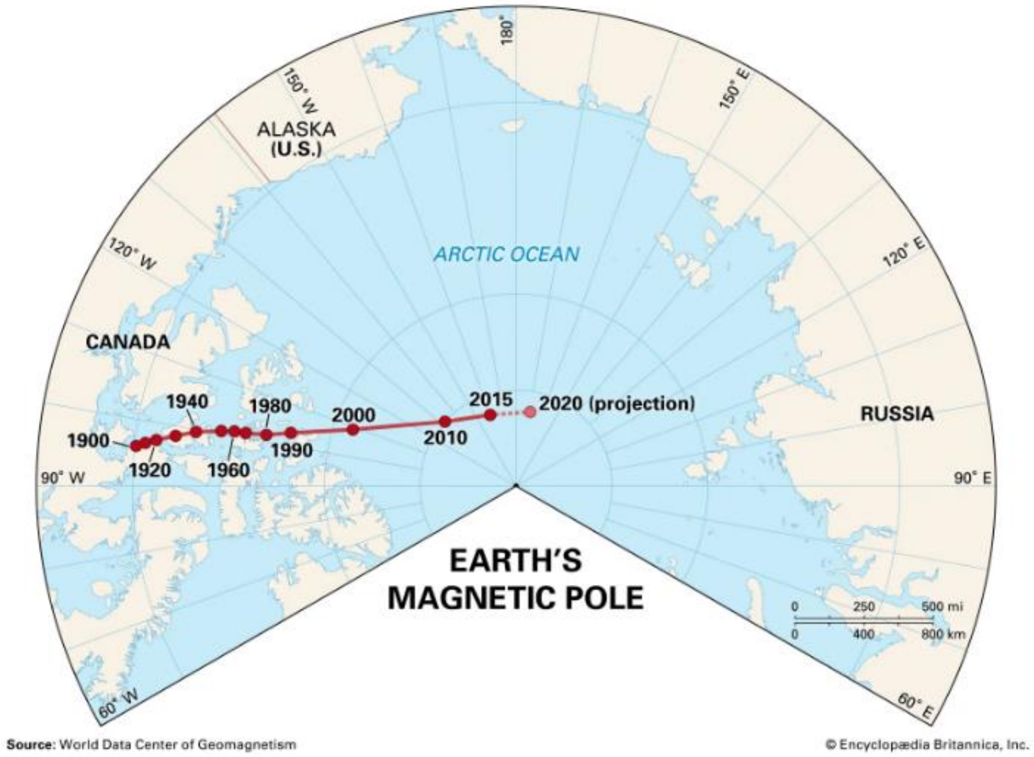

Figure 6: North Pole wondering. Taken from Encyclopaedia Britannica[16].

2. AIMS AND PRELIMINARY THOUGHTS

In chronological order, the project was intended* to achieve the following objectives:

i. Design and construct devices that spin and release an object and record its motion as it falls. The camera must be dropped nearly simultaneously with the observed body and with a similar fall rate to record it in its reference frame. This facilitates the analysis of the object's motion and reduces aberrations to the video such as parallax.

ii. Calculate the moments of inertia for a range of objects of varying mass, size, geometry, and mass distribution.

iii. Perform observations on the objects varying the angular speed and rotation axis at launch. If the effect takes place, measure the flipping duration (how long a flip lasts) and

[15] Buis, A. (2021). *Flip Flop: Why Variations in Earth's Magnetic Field Aren't Causing Today's Climate* Change. NASA. Retrieved 12th of August 2022 from https://climate.nasa.gov/ask-nasa-climate/3104/flip-flop-why-variations-in-earths-magnetic-field-arent-causing-todays-climate-change/

[16] The Editors of Encyclopaedia Britannica. *Polar Wandering*. Accessed August 31st 2022 at https://www.britannica.com/science/polar-wandering

the flipping period (the time between flips). There will be three groups of observed objects:

a) A variety of simple, rigid bodies used to get an estimate of the magnitudes of the measured quantities.
b) Solid spheres with exaggerated asymmetries (e.g., extra mass, deformations, protuberances, or a combination thereof). These are simplified models of a rigid Earth. The asymmetries are exaggerated because if we scale the dimensions of the Earth to the experiment the flipping time would be infinitely long. We intend to extrapolate our results from these exaggerated asymmetries back to the parameters of the Earth.

Figure 7: Potassium permanganate dissolving in a glass of water that has been recently spun retaining angular momentum. The picture has been edited to make the purple traces more noticeable

c) Spheres with similar asymmetries (and perhaps mass) to the solid ones but filled with water and powdered potassium permanganate. The latter dissolves in threads so it helps to visualise the motion of the water inside (fig. 7). Of particular interest would be first dropping frozen water-filled modified spheres and then dropping them when the water is liquid so that each object's geometry, mass, and its distribution (ignoring local small irregularities in the water mass distribution in both solid and liquid states) remain the same. Thus, we can more directly assess how Dzhanibekov's effect changes when the interior is liquid rather than solid.

iv. Plot graphs of the collected data of the flipping period and flipping duration vs angular momentum and vs the angular speed to reveal any dependences.

v. Model the influence of mechanical parameters (mass distribution, angular velocity, etc.) on Dzhanibekov's effect.

*As mentioned in the overview, many of these objectives needed to be adjusted. It proved impossible to make the camera fall with the exact same speed as the object so we could not trace the exact motion of the liquid inside bodies. Hence, the focus moved to exploring the dynamics of solid and liquid-filled bodies.

3. EQUIPMENT DESIGN & DEVELOPMENT

The equipment had to be designed and built because, at the time of the project, there were none already existing devices that could be used for our purposes. Most of the objects used for developing apparatus were modified and repurposed everyday objects. This was partly due to budget constrains but it meant an opportunity to exercise creativity and resourcefulness, valued skills for an experimental physicist.

Two devices were developed. First, a camera rail to guide a camera as it falls so its lens always aims at the falling spinning object and to make it fall alongside the object. Second, a launcher that spins and releases the object giving it as little lateral motion as possible, so that the object falls straight down with angular momentum purely about the vertical axis. We present the final versions of the devices. For all the prototypes see section 3-4 of the appendix.

3.1 The camera rail

This device consisted of three elements: the camera holder, the drop platform, and the base. These are all connected by fishing lines working as rails.

3.1.1 The camera holder

The holder (fig. 8) was designed to accommodate the GoPro HERO 5 camera inside its protective case (fig. 9).

Figure 8: Camera holder with the safety Velcro strap and the aerodynamic tip.

Figure 9: GoPro camera and its protective case. Notice that the lens protector was removed after it was cracked.

A cardboard and tape case was built corresponding to the dimensions of the protective case. Four metal tubes were placed on the respective corners, so the lines ran through them as the holder fell. A safety Velcro strap was added to stop the case with the camera from leaving the holder in case of a bounce back because such an accident damaged the protective case (fig. 9). A shampoo bottle cap was filled with clay and attached to the bottom of the holder to make it more stable and more aerodynamic.

We added a white background behind the falling object to make observations clearer.

3.1.2 The platform

Figure 10: The drop platform fixed to the handrail of the second floor at the School of Physics. The holder in the picture is not the final design produced.

A moveable drop platform (fig. 10) was designed, and manufacture was handled by the workshop at the university. Movability was needed to switch test locations if necessary and it was achieved with the small, squared wood plank, at the very left in fig. 10, that could be fixed in place using nuts and the long bolts extending from the main body of the platform. Eventually, this piece broke, and it was replaced with a metal piece. We also had to place some paper between the vertical plank and the handrail so that the main plank was perpendicular to the ground as a levelling bubble showed that the handrail was not perpendicular to it. These two modifications are in fig. 11. The bolts on the main plank held the four fishing lines in tension. The latter passed through four holes drilled in the main plank at locations corresponding to the tubes on the corners of the holder. A thread passed through a fifth hole, in the centre of the other four, and looped around the holder. This allowed to pull the camera holder back up after a drop.

Figure 11: The metal fixing plank and the paper used to correct for the handrail inclination.

3.1.3 The base

Figure 12: The base seen from above.

The base (fig. 12) was built on a wooden plank with magnetrons at its ends acting as weights. Wire terminal blocks (fig. 13) were screwed onto the plank (not visible in fig. 12) and held the bottom ends of the lines. A topless cardboard container provided a safety cushion with side sponge cloths (fig. 14) and a central one (not shown) that folded onto itself when the holder entered the container. These had to be reset after every drop. We placed a retractable tape measure under the container with its mouth exactly under the holder and attached thicker and stronger (primary) line (orange) to the wheel. This line was connected by a knot to a secondary line tied to the holder. By moving the vertical position of the knot, the amount of line coming out of the retractable tape measure was controlled. This is related to the number of turns on the torsion spring. Thus, we increased the downward force (at release) on the holder until it finally fell at the same rate as the object.

Figure 13: Wire terminal blocks. Image taken from RS Components.

[17] Phoenix Contact. *EC 6 3POL, Terminal Strip, 41A, Screw Terminals*. RS Components. Accessed August 28th at https://uk.rs-online.com/web/p/standard-terminal-blocks/8596348?cm_mmc=UK-PLA-DS3A-_-google-_-CSS_UK_EN_Fallback-_-All+Products-_-8596348&matchtype=&pla-293946777986&cq_src=google_ads&cq_cmp=9815220214&cq_term=&cq_plac=&cq_net=g&cq_plt=gp&gclid=Cj0KCQjwjbyYBhCdARIsAArC6LIw00pN5fsvZbNKVmCBYIKZx12_AI7fn9aYXpiVprTxZouz7POZuFcaAvIYEALw_wcB&gclsrc=aw.ds

Figure 14: Side sponge cloths and retractable tape measure inside cardboard container.

3.2 The launcher

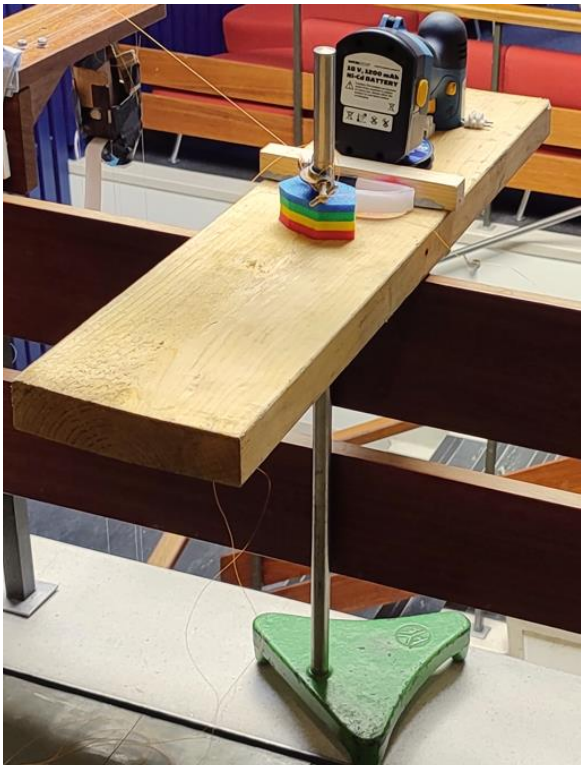

Figure 15: The launcher.

A drill provided the spin and release mechanism. Grabbing the chuck of the drill as it spun counterclockwise expanded the three-piece clamp it had instead of a drill head, releasing its load. For more stability, the drill was placed in a wooden plank, mounted on a stand, with a hole (fig. 15). It was secured employing wire terminals with bolts in them to adjust to the shape and orientation of the chuck (fig. 16) guaranteeing it was perpendicular to the ground with the help of a rectangular wooden prism supporting the handle. Extra screws under the plank impeded rotation about the stand pole.

Figure 16: Terminal blocks with bolts securing the drill.

Bubble wrap was placed below the launcher to protect the falling spheres.

Working with the devices required two people as one hand is needed for triggering the drill, one for dropping the camera and one for releasing the spinning object. These last two had to be done by the same person to be simultaneous.

4. RESULTS[18]

A code[19], developed by Dr Vorgul, was used to calculate the principal moments of inertia of the bodies we experimented with. For that purpose, the bodies' dimensions and weight (including those of the bodies' composite parts of different densities) were measured precisely and the shape was then digitised.

[18] It is worth mentioning that these observations were performed after my participation in the project had ended but using the equipment and method that I devised.

[19] Available at GitHub, https://github.com/Irena26/Moments-of-Inertia

4.1 Rotation and flipping of a key rotating around its minor momentum axis

Figure 17: Successions of frames from the flipping key video, and QR code for the video.

To calculate the predicted time before the flip, a period of oscillations for the solution of equation (2) with D given by (3) was calculated under the condition (6) for the MOI,

$$\tau = \frac{2\pi}{D(t=0)} \tag{7}$$

The value of D depends on ω_1 and ω_2 which we cannot know exactly, hence we use constrains for them, determined by that they need to be less than ω_3 since that is the angular velocity of the main rotation, and by (6). That gives us lower and upper estimates for the time before flipping.

The results of the modelling and the experiment are summarised in Table 1.

Result for the key	Calculated	Measured
Frequency of rotation, ω_3	N/A	$21.08058\ \mathrm{Hz}$
Moments of inertia	$A = 6.348 \times 10^{-4}\ \mathrm{kg\,m^2}$ $B = 6.534 \times 10^{-4}\ \mathrm{kg\,m^2}$ $C = 2.76 \times 10^{-4}\ \mathrm{kg\,m^2}$	N/A
Time till the flip	$\tau > 1.90954\ \mathrm{s}$ $\tau < 3.711\ \mathrm{s}$	$\tau = 2.60\ \mathrm{s}$

Table 1: Calculated and measured results for flipping key.

It is seen clearly that the measured timing falls within the theoretical calculated constrains, and the experiment showed the key flipping. That confirms that objects rotating around their minor axis can experience Dzhanibekov's effect, and the quasi-linear theory correctly estimates its timing.

4.2 Rotation and flipping of a sphere with ice/water and asymmetric weights

a)

b)

c)

d)

Figure 18: Successions of frames from the videos of a flipping solid sphere (a) and a sphere filled with about 90% ice and about 10% water (d), and solid (b) and partially liquid-filled (c) spheres videos QR codes

As explained in section 2, we exaggerated the asymmetry in the experiment, aiming at extrapolating the results towards lower asymmetry. The solid ball had density close to that of the water and ice sphere, and was of a similar size.

The results show a good fit of the theoretical timing to the observed one. The ball flipped in both cases. To our surprise, the one with some liquid started flipping a bit earlier than the solid one. It is not a fully valid comparison though, since the spheres were slightly different, and there was a small leak in the liquid-filled sphere.

Result for the spheres		Calculated	Measured
Solid sphere with 'wings'	Frequency of rotation, $\boldsymbol{\omega_3}$	N/A	$1110.1\ \text{Hz}$
	Moments of inertia	$\mathrm{A} = 6.01634 \times 10^{-10}\ \mathrm{kg\ m^2}$ $\mathrm{B} = 6.1548 \times 10^{-10}\ \mathrm{kg\ m^2}$ $\mathrm{C} = 2.5025 \times 10^{-10}\ \mathrm{kg\ m^2}$	N/A
	Time till the flip	$\tau > 0.0068\ \mathrm{s}$	First flip $\tau = 0.01415\ \mathrm{s}$
		$\tau < 0.0316\ \mathrm{s}$	Second flip $\tau = 0.01321\ \mathrm{s}$ after 1st flip's start
Sphere with 'wings' filled with 90% ice core and 10% water	Frequency of rotation, $\boldsymbol{\omega_3}$	N/A	$966.6438\ \text{Hz}$
	Moments of inertia	$\mathrm{A} = 6.01634 \times 10^{-10}\ \mathrm{kg\ m^2}$ $\mathrm{B} = 6.1548 \times 10^{-10}\ \mathrm{kg\ m^2}$ $\mathrm{C} = 2.50255 \times 10^{-10}\ \mathrm{kg\ m^2}$	N/A
	Time till the flip (as if solid)	$\tau > 0.0078165\ \mathrm{s}$	First flip $\tau = 0.008973\ \mathrm{s}$
		$\tau < 0.036318763\ \mathrm{s}$	Second flip $\tau = 0.0166667\ \mathrm{s}$ after 1st flip's start

Table 2: Calculated and measured results for flipping solid and partially liquid-filled spheres.

4.3 Rotation and semi-flipping of an asymmetric spherical capsule filled with oil

Figure 19: QR code for half-flipping rotating spherical capsule filled with oil

A small asymmetric plastic capsule filled with oil performed half-a-flip and then returned to its original position of rotation. Comparing to the results in 4.2, one can conclude that viscosity and density of the liquid influence the way Dzhanibekov's effect manifests itself.

4.4 Calculating timing constrains for the Earth

With the moments of inertia of the Earth as in section 1.3, using the rotation frequency of

$$\omega = \frac{2\pi}{24\ \mathrm{h} \cdot 60\ \mathrm{min} \cdot 60\ \mathrm{s}} = 0.000072722\ \mathrm{Hz}$$

the lower constrain for the time between flipping can be estimated as

$$\tau = \frac{2\pi}{\sqrt{\frac{(B-A)(B(B-C)-A(A-C))}{ABC}\omega^2}} = 3468293956.104247\ \mathrm{s} = 109.98\ \mathrm{years}$$

Since the Earth is rotating around its major axis, there are no second constrains on the rotational frequencies around other axis, hence there is no way to calculate the upper constrains.

5. CONCLUSIONS

To summarise the results, it was discovered that Dzhanibekov's effect can happen when a body is rotating around its minor or major axis (though conventional assumption says that it cannot), which applies to the case of how the Earth is rotating.

Experimental results showed good agreement in timing with our quasi-linear theory calculations. This allows to estimate the lower limit for the time between two possible flip-like events, which came to be as low as around 110 years. The experimental results show that a body partially filled with liquid can flip too but depending on the parameters of the liquid and other parts of the body, this flip could be either complete or incomplete. In any case, the liquid inside the body would be affected, which in the case of the Earth would result in some changes to the global magnetic field.

With this pilot research, we aimed to get the first insight into the problem. The results are pre-requisites for further research and could lead to a new direction of research into the Earth dynamic, magnetic field, and climate change.

6. REFERENCES

Ashbaugh, M. S., Chicone, C. C., and Cushman, R. H. The Twisting Tennis Racket. *Journal of Dynamics and Differential Equations*, 1991; 1, (Vol. 3), pp 67-85. DOI: 10.1007/BF01049489

Buis, A. (2021). *Flip Flop: Why Variations in Earth's Magnetic Field Aren't Causing Today's Climate* Change. NASA. Retrieved 12th of August 2022 from https://climate.nasa.gov/ask-nasa-climate/3104/flip-flop-why-variations-in-earths-magnetic-field-arent-causing-todays-climate-change/

Chandler, B., Frost, D.A, Lasbleis, M. and Romanowicz, B. Dynamic history of the inner core constrained by seismic anisotropy. *Nature Geoscience,* 2021; (**Vol. 14**), pp 531–535. DOI: 10.1038/s41561-021-00761-w

Chen, W. and Shen, W.B. New estimates of the inertia tensor and rotation of the triaxial nonrigid Earth. *Journal of Geophysical Research*, 2010; B12, (**Vol. 115)**. DOI: 10.1029/2009JB007094

Daradich, A., Gomez, N., Matsuyama, I. and Mitrovica, J. X. The rotational stability of a triaxial ice-age Earth. *Journal of Geophysical Research Atmospheres,* 2010; BO5401, (**Vol. 115**). DOI: 10.1029/2009JB006564

Daradich, A., Gomez, N., Matsuyama, I. and Mitrovica, J. X. The rotational stability of a triaxial ice-age Earth. *Journal of Geophysical Research Atmospheres,* 2010; BO5401, (**Vol. 115**). DOI: 10.1029/2009JB006564

Garelli, L., Storti, M. and Trivisonno, N. The Tennis Racket Theorem, Analysis and Numerical Simulation of the Intermediate Axis Theorem. *Mecánica Computacional*, 2021; (**Vol. 28**), pp. 1353-1365.

GEOLOGYSCIENCE. The Earth's Layers. Accessed August 12th 2022 at https://geologyscience.com/geology-answer/the-earths-layers/

Gorbunov, A., Kozhevnikov, M., Olesya, B. and Royan, J. The Role of Immersivity in Three-Dimensional Mental Rotation. *Design Computing and Cognition*, 2008, pp.143-157. DOI: 10.1007/978-1-4020-8728-8_8

Petrov, A. G. and Volodin, S. E. Janibekov's Effect and the Laws of Mechanics. *Doklady Akademii Nauk*, 2013; 4 (**Vol. 451**), pp. 399–403. DOI: 10.1134/S1028335813080041

Phoenix Contact. *EC 6 3POL, Terminal Strip, 41A, Screw Terminals*. RS Components. Accessed August 28th at https://uk.rs-online.com/web/p/standard-terminal-blocks/8596348?cm_mmc=UK-PLA-DS3A-_-google-_-CSS_UK_EN_Fallback-_-All+Products-_-

8596348&matchtype=&pla-293946777986&cq_src=google_ads&cq_cmp=9815220214&cq_term=&cq_plac=&cq_net=g&cq_plt=gp&gclid=Cj0KCQjwjbyYBhCdARIsAArC6LIw00pN5fsvZbNKVmCBYIKZx12_AI7fn9aYXpiVprTxZouz7POZuFcaAvIYEALw_wcB&gclsrc=aw.ds

Plasma Ben. Published 3 of March 2009. Dancing T-handle in zero-g, HD. [Video]. YouTube.com. https://www.youtube.com/watch?v=1n-HMSCDYtM

Sarkar, D. (2021). *Earth has been hiding a fifth layer in its inner core*. Astronomy. Accessed August 12th 2022 at https://astronomy.com/news/2021/03/earth-has-been-hiding-a-fifth-layer-in-its-inner-core

ThatsMaths. (2019). The Intermediate Axis Theorem. Accessed August 12th 2022 at https://thatsmaths.com/2019/12/12/the-intermediate-axis-theorem/

The Editors of Encyclopaedia Britannica. *Dynamo Theory*. Accessed August 13th 2022 at https://www.britannica.com/science/dipolar-hypothesis

The Editors of Encyclopaedia Britannica. *Polar Wandering*. Accessed August 31st 2022 at https://www.britannica.com/science/polar-wandering

7. APPENDIX

7.1 The Intermediate Axis Theorem

For a body with $I_3 > I_2 > I_1$ and in force free motion ($M_1, M_2, M_3 = 0$), Euler's Equations for a rigid body become:

$$I_1\dot{\omega_1} = (I_2 - I_3)\omega_2\omega_3$$
$$I_2\dot{\omega_2} = (I_3 - I_1)\omega_3\omega_1$$
$$I_3\dot{\omega_3} = (I_1 - I_2)\omega_1\omega_2$$

Supposing spin about axis 1 so $\omega_1 \gg \omega_2, \omega_3$ then $I_1\dot{\omega_1} \approx 0$ making ω_1 approximately constant. Thus,

$$\dot{\omega_2} = \frac{(I_3 - I_1)\omega_1}{I_2}\omega_3 = k_2\omega_3$$
$$\dot{\omega_3} = \frac{(I_1 - I_2)\omega_1}{I_3}\omega_2 = k_3\omega_2$$
$$\ddot{\omega_2} = k_2\dot{\omega_3} = k_2k_3\omega_2$$
$$\ddot{\omega_3} = k_3\dot{\omega_2} = k_2k_3\omega_3$$

where k_2 and k_3 are constants. Because $k_2 k_3 < 0$, these are oscillatory solutions around $\omega_2, \omega_3 = 0$, so this rotation is stable. This is also true for spin about axis 3 but if we repeat this process with axis 2, we get:

$$\ddot{\omega_1} = \lambda_1 \lambda_3 \omega_1$$
$$\ddot{\omega_3} = \lambda_1 \lambda_3 \omega_3$$

Where

$$\lambda_1 = \frac{(I_2 - I_3)\omega_2}{I_1}$$
$$\lambda_3 = \frac{(I_1 - I_2)\omega_2}{I_3}$$

$\lambda_1 \lambda_3 > 0$ giving an exponential growth of ω_1 and ω_3 so this motion is unstable.

7.2 Quasi-linear approach

$I_1, I_2, I_3 = A, B, C$. Assume a rotation about the axis corresponding to C and effective torques with respect to the origin M_1, M_2, M_3 including torques from fictitious forces.

From Euler's equations:

$$B\omega_2\{A\dot{\omega_1} + (C - B)\omega_2\omega_3\} = M_1 B\omega_2$$

+

$$A\omega_1\{B\dot{\omega_2} + (A - C)\omega_1\omega_3\} = M_2 A\omega_1$$

=

$$AB\frac{d}{dt}(\omega_1\omega_2) + [B(C - B){\omega_2}^2 + A(A - C){\omega_1}^2]\omega_3 = M_1 B\omega_2 + M_2 A\omega_1$$

and

$$\frac{d}{dt}\{C\dot{\omega_3} + (B - A)\omega_1\omega_2\} = C\ddot{\omega_3} + (B - A)\frac{d}{dt}(\omega_1\omega_2) = \dot{M_3}$$

Rearranging terms and substituting $\frac{d}{dt}(\omega_1\omega_2)$, we obtain a quasi-linear equation ω_3:

$$\ddot{\omega_3} - \frac{B - A}{ABC}[B(C - B){\omega_2}^2 - A(A - C){\omega_1}^2]\omega_3 = \frac{\dot{M_3}}{C} - \frac{(B - A)(M_1 B\omega_2 + M_2 A\omega_1)}{ABC}$$

7.3 Bracket rails

The first rails were made to guide a smartphone and included two long, parallel, bracket ([ ) shaped structures that would guide its fall, hence the name.

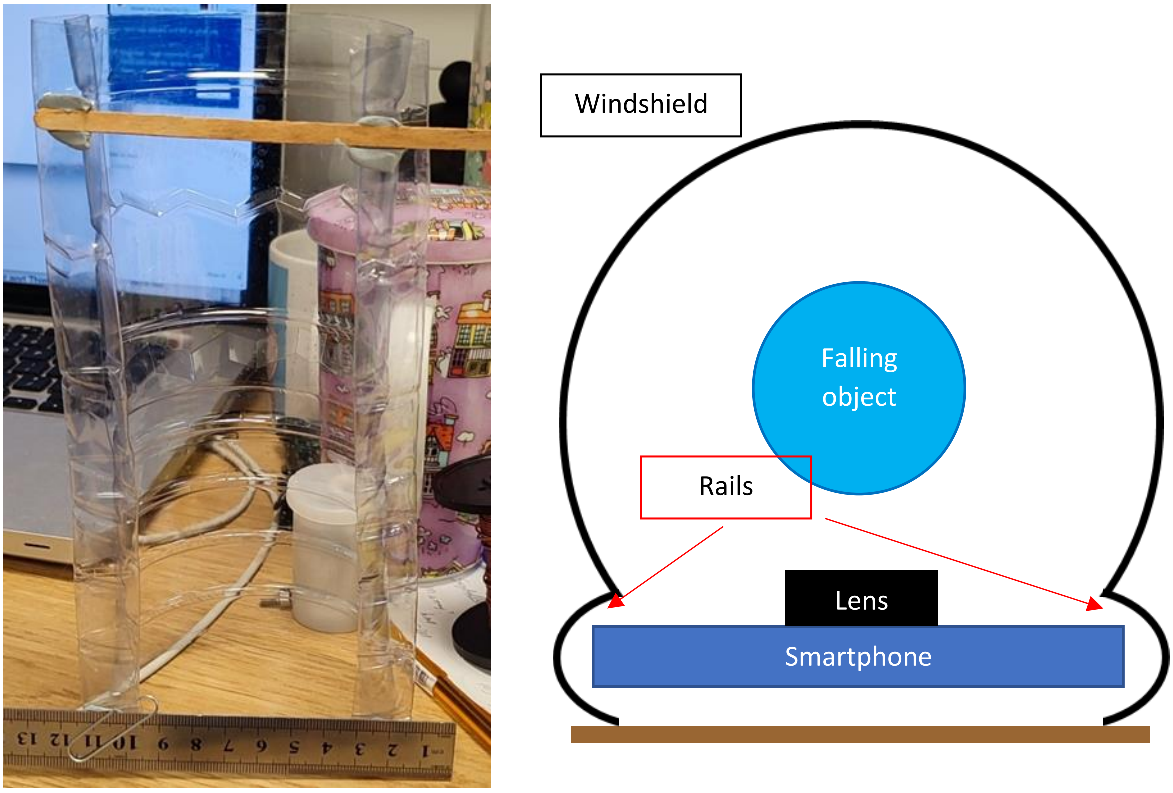

Figure 20: Bottle bracket-rail prototype (left) and a top view diagram showing how it works (right).

The first design (fig. 20) was made of a cut-open and bent plastic bottle with makeshift crossbars to adjust the aperture width. The rails fit the width and thickness of the smartphone. A protective case – a bag made of packaging foam – helped to avoid scratching the phone's glass surfaces with the sharper plastic ends. The unbent part of the bottle shielded falling objects from wind currents, further strengthening the experimental method. The plan was to make several of these and pile them up on top of each other producing a structure many meters tall. However, too many bottles were required for this.

The second design (fig. 21) was more simply produced. It was just a wide strip of cardboard bent into a bracket shape (as seen from the top) with some crossbars fixed across to maintain its shape. Once more, several of these were to be made and put together one of top of the other. However, an external skeleton to stop it from collapsing would have been necessary. This was never done because this line of rails was abandoned after a preliminary recording was attempted revealing that friction slowed down the fall of the camera by a lot and resulting in a cracked phone screen protector. Consequentially, we switched to a different recording device that would be less easily damaged. Luckily, a fellow Laidlaw scholar offered to lend us his GoPro Hero 5 camera for the project.

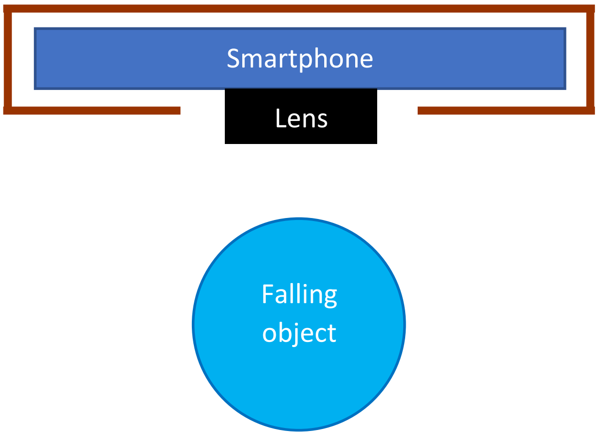

Figure 21: Cardboard bracket-rail prototype (left) and a top view diagram showing how it works (right).

7.4 String rails

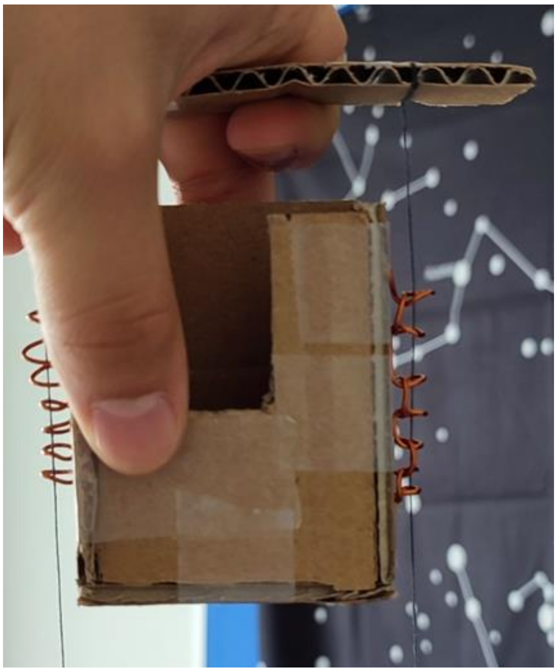

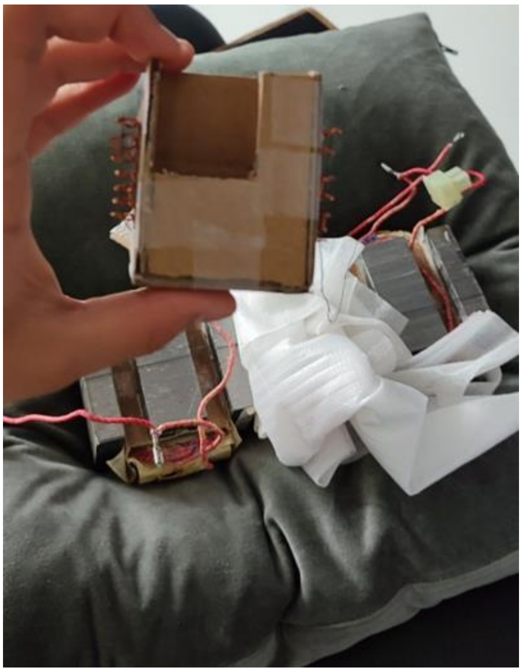

Figure 22: First string-rail cardboard holder (left and right front) and its base (right back).

The second generation of rails employed strings and some pipes through which these would run as the camera (in a holder) fell. The first holder had copper wires bent into loops attached to its sides through which we passed sewing threads (fig. 22). At the base, the threads were tied to two magnetrons, originating from a broken microwave, that kept the threads at a fixed location and distance from each other and constrained the foam wrap used to break the fall safely in combination with the pillow under it. This design resulted in wobbly recordings because the hoops were too wide and too far apart from each other and the threads snapped easily.

The wires and threads were replaced with thin metal tubes and fishing line that the workshop at the School of Physics provided. We placed a tube at each corner for greater stability. The foam was removed and instead loops were attached to the pillow to redirect the fishing lines to the magnetrons no longer on the pillow (fig. 23).

Figure 23: Second string-rail prototype. Top view of the camera in the holder on top of the pillow.

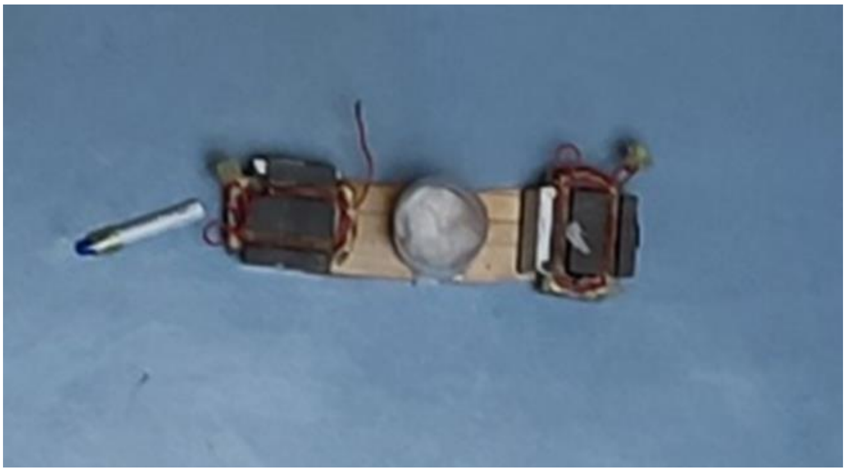

Figure 24: Top view of the third string-rail base.

The pillow at the base was removed after it was judged too thin to break a ~ 4 m drop. Instead, the magnetrons were placed at the ends of a thin wooden plank to hold it in place (fig. 24) and wire terminal blocks were screwed to the plank at locations corresponding to the four metal tubes of the holder and were used to secure the bottom ends of the lines. A plastic bottle, with its ends cut off, was placed over the terminals with the lines passing through its cross-section and was filled with torn pieces of packaging foam to work as a cushion.

After several drops, the packaging foam was moulded into a quasi-solid blop, which risked damaging the camera, so the bottle was filled with small polystyrene balls. These were replaced with torn pieces of sponges as the balls would fly away at impact. However, after each drop, the sponges began to tightly arrange themselves in such a way that exerted a lateral force on the lines making them no longer parallel all the way down. Furthermore, we replaced the fishing lines with stronger, thicker, orange ones and the protective case for the camera that we had ordered finally arrived, so we made a bigger holder and had to drill new holes on the main plank. This all resulted in a slower fall for the camera and holder. We tried to attach a propeller to the top of the holder to increase its downward speed, but this proved difficult to control.

Consequentially, we returned to the thinner lines, and removed the bottle. Instead, we hung sponges on the lines (fig. 25) with incisions so that they would not push the lines apart. This set up had to be rearranged after every drop which slowed down the time between drops to several minutes. In one such drop, the holder bounced up launching the camera a few meters away breaking glass protecting the lens. For safety, we added the white Velcro strap to the holder and a cardboard container to the base. Yet, the sponges would become stuck in the container after a drop pushing the lines a part again.

(From here on, the camera rail became what is shown in section 3.1).

Figure 25: Hanging-sponges cushion.